Research article

High-resolution magic angle spinning 1H NMR measurement of ligand concentration in solvent-saturated chromatographic beads

Fredrik Elwinger[a,b] and István Furó[a]*

A method based on 1H high-resolution magic angle spinning NMR has been developed for measuring concentration accurately in heterogeneous materials like that of ligands in chromatography media. Ligand concentration is obtained by relating the peak integrals for a butyl ligand in the spectrum of a water-saturated chromatography medium to the integral of the added internal reference. The method is fast, with capacity of 10 min total sample preparation and analysis time per sample; precise, with a reproducibility expressed as 1.7% relative standard deviation; and accurate, as indicated by the excellent agreement of derived concentration with that obtained previously by 13C single-pulse excitation MAS NMR. The effects of radiofrequency field inhomogeneity, spin rate, temperature increase due to spinning, and distribution and re-distribution of medium and reference solvent both inside the rotor during spinning and between bulk solvent and pore space are discussed in detail. © 2016 The Authors *Magnetic Resonance in Chemistry* published by John Wiley & Sons, Ltd.

Introduction

The ligand concentration in chromatography media is an important factor during their preparation and, ultimately, for their performance.[1,2] In a previous paper, single-pulse excitation magic angle spinning (SPE-MAS) 13C NMR was presented as a method to measure the concentration of butyl ligands in Butyl Sepharose™ High Performance medium.[3] The method was shown to have several advantages over conventional analytical procedures, often requiring cleavage of the ligand from the resin (here and henceforth the medium before chemical coupling of linker and ligand is called resin) or hydrolysis of the medium prior to analysis.[4–8] The developed 13C SPE MAS NMR protocol[3] yielded good reproducibility (relative standard deviation around 2%), but the low 13C SPE sensitivity lead to a total sample preparation and experimental time that amounts to several hours (at least seven or ten, depending on the selected protocol). Here, a high-resolution magic angle spinning (HR-MAS) 1H NMR protocol is described in the same medium with far shorter experimental times than the 13C method. As we are going to show, the two methods yield the same ligand concentration that validates both of them as accurate tools. As is the case for the 13C SPE MAS NMR,[3] one expects that the method presented here is more general and assumedly more accurate than those more conventional approaches that require chemical cleavage steps.[4–8] Regarding in general quantitative NMR[9–11] but in heterogeneous media, the relative performance of various methods is indeed an interesting issue, in particular for high-throughput analysis.

1H HR-MAS is often cited as capable to obtain well-resolved 1H NMR spectra in semi-solids, such as in a solvent-swollen medium,[12–22] where MAS suppresses line broadening caused by chemical shift anisotropy and/or by magnetic field inhomogeneity, both often left at least partially un-averaged.[23] Quantitative

HR-MAS measurements require suitable reference that may be substances dissolved in the swelling solvent,[24–27] the solvent itself,[28] added macromolecular components[29] that can take the form of silicon plugs,[30,31] or the resin itself.[27,29,32,33] In addition, one may employ electronically produced reference signals, such as in the ERETIC™ method.[24,34–37] All these can be considered as internal references. While it is also possible to use an external reference, an internal reference is preferred because that usually leads to more accurate results, for example, because random errors caused by instrument instability or sample positioning are canceled. Using the solvent as reference is possible only if the amount of solvent in the sample can be determined, which may not be the case or can take additional time. Referencing to the signal of the solid component might be a good choice, if that signal is available at all and well resolved and is not sensitive to varying experimental conditions like the sought concentration itself. If one uses instead another solid component like a silicon plug as reference material, the sample and the reference are not distributed in the same manner in the coil volume, which can be a problem because of RF inhomogeneity.[38–40] An uneven distribution of the sample within the rotor and

---

* Correspondence to: István Furó, Division of Applied Physical Chemistry, KTH Royal Institute of Technology, Teknikringen 36, SE-10044 Stockholm, Sweden. E-mail: furo@kth.se

a   Division of Applied Physical Chemistry, KTH Royal Institute of Technology, Stockholm, Sweden

b   GE Healthcare Bio-Sciences AB, Uppsala, Sweden

thereby coil is also a problem for the ERETIC method, which in addition requires manual adjustments of the phase and frequency for each new sample being analyzed, thereby making high-throughput analysis difficult. As a remaining option, a reference based on a substance dissolved in the swelling solvent must satisfy certain conditions; it should be stable, provide a well-resolved peak in the spectrum, and preferably have a short longitudinal relaxation time, T_1. As we are going to show later, selectively deuterated 3-(trimethylsilyl)propionic acid (TMSP) is a suitable reference compound, and by using that and an appropriate experimental protocol, we can achieve an accuracy of <2% when obtaining ligand concentration in a hydrated chromatography medium.

Experimental

Materials

The Butyl Sepharose High Performance chromatography medium was from GE Healthcare. A schematic structure of the butyl ligand coupled to Sepharose High Performance resin is shown in Fig. 1. 3-(trimethylsilyl)propionic-2,2,3,3-D$_4$ acid sodium salt (98.8% D, chemical purity >99.9% determined by ^{1}H NMR), and D$_2$O (99.9% D) were from Cambridge Isotope Laboratories.

Preparation of sample

The medium was washed with a very large extent of distilled water and then with D$_2$O (three times) on a glass filter with vacuum suction in-between the washing steps. This procedure removed the storage solution and, as much as possible, the ^{1}H water background. Thereafter, two sample preparation pathways were followed. In the first pathway, called pathway A, three additional washing steps followed with a reference solution of 0.1000 (±0.0004) M TMSP in D$_2$O. Then, a special sample preparation tool manufactured for this purpose[3] was used to compact a tightly packed bed of beads of a well-defined volume of 50.0 (±0.16) μl. In essence, the preparation tool consists of a cylinder of well-defined volume, where the bead pack is formed by low-vacuum suction. In real chromatography columns, the medium is usually packed and compressed (typically by 10–20%) by a variety of methods and kept compressed by enclosure. In the preparation tool used here, the medium is not compressed. The diameter of the bead plug (2.5 mm) matched exactly the diameter of the MAS rotor, and during preparation, the solution from between the beads of ~35 μm size was removed by low-vacuum (~260 mbar, not affecting the liquid within the bead pores that, with <100 nm maximum size, exert a high retaining capillary pressure on the wetting solvent) suction. The plug was then transferred to the MAS rotor and encapsulated there with proper spacing inserts. We note that for this sample preparation pathway, quantitative results demand that TMSP does not interact with the medium because interaction may change the distribution of TMSP between the pore space and the bulk liquid between the beads. For this preparation pathway, calculation of the ligand concentration (Section 2.3) requires
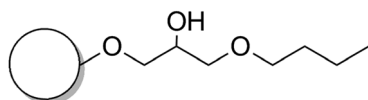

Figure 1. The ligand and linker to the agarose resin in the Butyl Sepharose High Performance chromatography medium.

the dry matter content of medium per volume, which was established by drying and weighing of a bead pack prepared as described earlier but without the additional washing steps with TMSP reference solution.

In the other sample preparation pathway, called pathway B, a compacting tool like the one earlier but larger provided a tightly packed bed of beads (diameter 7.0 mm) with a volume of 1.000 (±0.005) ml. Thereafter, a slurry of medium was prepared by mixing the bead plug with 0.938 (±0.003) ml of 0.1000 (±0.0004) M TMSP in D$_2$O. After careful mixing with a vortex mixer, 10.0 μl (with a precision of ~0.3%) of the mixer slurry was transferred to a MAS rotor using a micropipette. A distinct advantage with this sample preparation pathway is that there are no washing steps and no bulk liquid is removed from the slurry. Therefore, the reference TMSP signal is not influenced by having a significant interaction between TMSP and the matrix.

NMR measurements

The experiments with 4 mm MAS rotors (spin rates from 5 to 17.5 kHz) were performed on a Bruker 500 MHz Avance II spectrometer equipped with an HR-MAS probe. A single-pulse ^{1}H experiment was used with the 90° pulse length (~6.5 μs) accurately calibrated at each spin rate. The B_1 field produced by RF coils is inhomogeneous both in axial and radial directions.[38–40] The axial field inhomogeneity in the 4 mm probe used here was quantified by optimizing RF pulse length and acquiring spectra for a 1-mm thick rubber disk placed between two KelF inserts of varied length inside the rotor. The obtained axial RF field strength and integral intensity profiles vary in proportion to each other as is expected[35,36] from the well-known reciprocity principle[41] with maximum sensitivity in the middle of the rotor.

The recycle time was set to 25 s (at least five times T_1 at any circumstance) where T_1 was the longitudinal relaxation time for the TMSP peak ($T_1 = 4.1$ s) measured by inversion recovery (the ligand peaks used for quantification exhibited faster relaxation, $T_1 = 1.7$ s for the methyl and $T_1 = (1.4$–$1.5)$ s for the various methylene groups). The signal was acquired with four scans with the spectral width set to 200 ppm, and the transmitter frequency slightly off to the TMSP peak position. The signal was digitized into 256 k points with acquisition time of 1.31 s. Prior to Fourier transformation, exponential apodization by 3 Hz line broadening was applied. The obtained spectra (Fig. 2) were subject of linear baseline correction (more complex baseline correction schemes were found to introduce bias) in the ligand/reference spectral range.

The integration intervals are shown in Fig. 2c for the CH$_3$-CH$_2$-CH$_2$- moiety of the butyl ligand (integral I_{butyl} with seven protons) and for the TMSP (integral I_{TMSP} with nine protons). From those integrals, the ligand concentration, c_{butyl} [μmol/ml medium], was calculated as

$$c_{butyl} = \frac{9}{7} \times \frac{n_{TMSP}}{V_{medium}} \times \frac{I_{butyl}}{I_{TMSP}} \qquad (1)$$

where, for pathway B, n_{TMSP} [μmol] and V_{medium} [ml medium] refer to the amount of TMSP respective the volume of medium *in the prepared slurry*, that is, *not* the amount in the MAS rotor. Hence, the obtained result is insensitive to small differences in rotor packing. n_{TMSP} is calculated from the volume of TMSP solution used to prepare the slurry and the concentration of that solution, while V_{medium} is the exactly defined internal volume of the packing tool used for preparing the bead pack (Section 2.2). For pathway A,
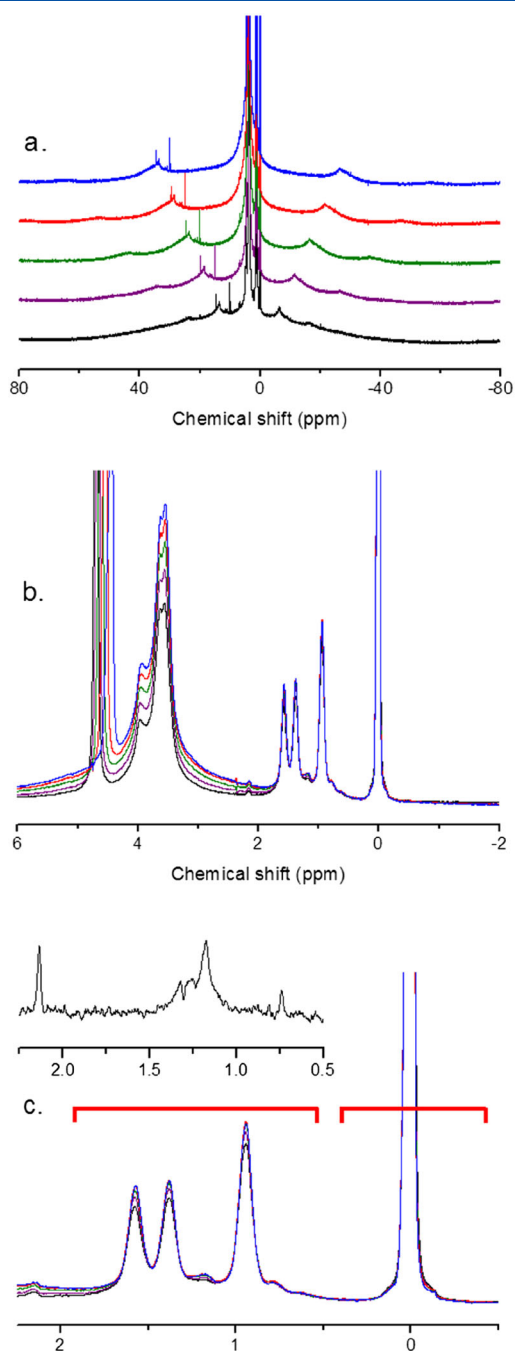
V_{medium} is as previously mentioned, while n_{TMSP} can be estimated under the assumption of identical concentration of TMSP in the pore volume and in the bulk from the mass of medium saturated with TMSP solution in the rotor and the dry matter content of medium per volume.

We stress here that this mode of calculation provides the ligand volume concentration in the bead pack prepared as specified in Section 2.2. In real columns, compression (different for different type of columns) renders the ligand volume concentration higher. The scaling factor between the volume concentration here and in real columns is exactly the ratio of the respective dry matter contents per volume.

Results

The effect of molecular mobility in dry and hydrated samples

Previously,[3] we investigated dry samples where compressing the medium provided maximum signal intensity for ^{13}C. For ^{1}H with its much higher signal intensity, one may obtain suitable signal even without compaction. Hence, the first question to decide is whether dry or wet medium is most suitable for quantitative experiments. Spectra were acquired at different MAS spin rates for wet samples where the TMSP solution between the beads was removed by low-vacuum suction (Fig. 2) and for dry medium (Fig. 3). As is clear from the strong sidebands in Fig. 3a, in the dry sample,
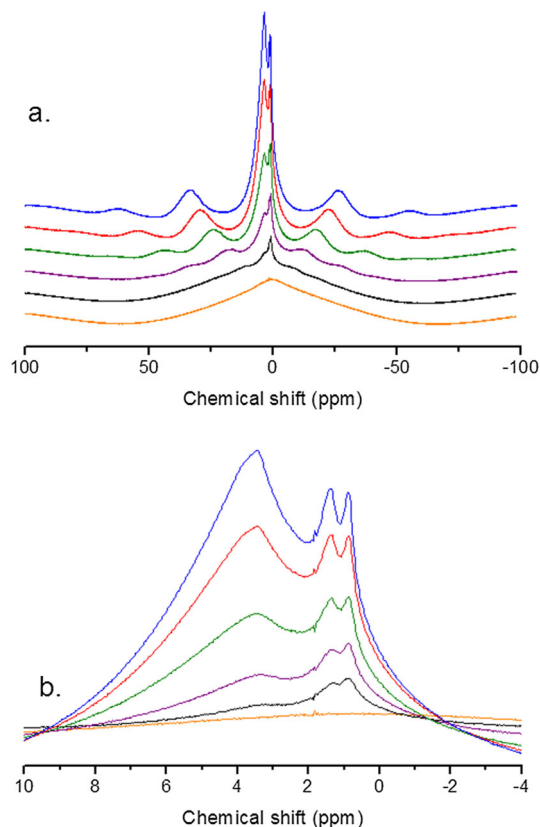

Figure 2. ^{1}H high-resolution MAS spectra at different magic angle spin rates of fully hydrated chromatographic beads. Spin rates in Hz: 5000 (black), 7500 (purple), 10 000 (green), 12 500 (red), and 14 500 (blue). (a) The whole spectral range. The 3-(trimethylsilyl)propionic acid (TMSP) peak is cut at ~7% of the peak amplitude. (b) Magnification of the significant spectral range with the center bands. Chemical shifts: 0 ppm (TMSP), 0.95 ppm (-CH$_3$ in butyl), 1.4 and 1.6 ppm (-CH$_2$CH$_2$- in butyl), 2.5–4.0 ppm (-OCH$_2$- in butyl and agarose), and 4.7 ppm (water). The water signal is shifted to lower chemical shift with increasing spin rate as a result of the temperature increase in the rotor. The TMSP peak is cut at ~30% of the peak amplitude. (c) Magnification of the ligand spectral range. Information about concentration was obtained by spectral integration over ranges as shown. The baseline in the ligand and reference spectral ranges was corrected in conjunction to the integration. There are a number of small peaks in the butyl integration region that are not due to the ligand. The inset shows a spectrum for resin (prior to coupling of the linker and ligand) with TMSP. The two peaks at 0.74 and 2.14 ppm are due to non-deuterated methylene groups in TMSP. The other peaks come from chemical groups on the resin.

Figure 3. ^{1}H high resolution MAS spectra at different magic angle spin rates of dry medium. Spin rates in Hz: 0 (orange), 5000 (black), 7500 (purple), 10 000 (green), 12 500 (red), and 14 500 (blue). (a) The whole spectral range (note the vertical offset). (b) Magnification of the significant spectral range. The agarose peak (~4 ppm) and the ligand peaks (0–2 ppm) are not well separated.

the spinning rate is not sufficiently high to suppress homonuclear dipolar couplings. In addition, the central lines from resin and ligand are broad and overlapping, making the determination of resolved spectral integrals very difficult and certainly model sensitive (if performed by fitting).

In the wet beads, the agarose signal provides discernible sidebands (Fig. 2a) and significantly increases its central peak intensity (Fig. 2b) in the whole explored range of spinning speed. Hence, the agarose signal cannot be used as internal reference for quantitative experiments, and therefore, we had to rely on TMSP added to the solvent. Water, TMSP, and the butyl ligand also provide spinning sidebands but only on the high-chemical shift side, which indicates an asymmetric line shape for them because of magnetic field inhomogeneity originating from the beads around[42] and/or chemical shift anisotropy. The sideband and central band intensities for these molecules vary on the same proportional manner with increasing spinning speed. Moreover, the spinning sideband intensity for all of them is below 1% of the central band intensity at spinning speeds above 5 kHz. Thus, as is further discussed in Section 3.3, spectral integrals of the ligand peaks in relation to that of the reference peak are expected to provide an accurate measure of ligand concentration at sufficiently high spinning rates. The integral regions for the butyl and TMSP peaks are shown in Fig. 2c. In the following sub-sections, we detail the additional steps that must be taken to obtain accurate integrals and thereby concentrations.

Factors influencing the signal intensity in MAS experiments

During the course of developing this protocol, we encountered variation of signal intensity both by spinning time and spinning speed. Identifying and eliminating those effects were the major part of this work.

3.2.1 Spatial re-distribution of sample components

In preliminary experiments, various ways to add the TMSP reference to the medium were tested. We typically observed that the intensity of the TMSP signal in the spectrum was changing a lot (up to 15%) both with time during spinning and with increasing spin rate. This was attributed to selective re-distribution of the reference solution and the beads within the rotor owing to the higher density of medium filled with solution compared with the density of free reference solution. Because the RF field is inhomogeneous within the coil, this explains the observation of non-constant TMSP intensity through the reciprocity principle.[41] As a control, a rotor completely filled with TMSP solution presents no time-dependent signal intensity.

The two possible solutions are (i) to limit the sample volume so that an inhomogeneous distribution of beads and solution are within a volume over which the RF inhomogeneity is small, as in pathway B; and (ii) to make samples so that the reference solution distribution closely follows that of the beads, as in pathway A. As concerning option (ii), it can be explored by equilibrating the beads in TMSP solution and then removing the solution from the regions between the beads by low-vacuum suction. Under the assumption that the solution is kept in the pores by capillary pressure and that TMSP has no significant interaction with the matrix, TMSP and ligand experience the same spatial distribution. Indeed, in samples prepared by following either pathway A or B, the TMSP and ligand signals were found to be constant during long spinning periods, as is specifically illustrated in Fig. 4 for pathway A.
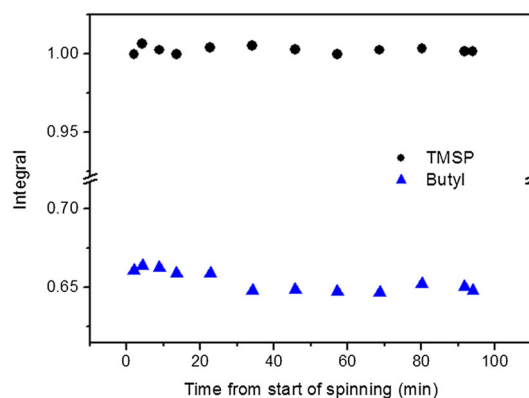

Figure 4. Normalized signal integrals for 3-(trimethylsilyl)propionic acid (TMSP) and ligand at 5 kHz spinning rate as a function of spinning time from start. The sample was prepared via pathway A (Preparation of sample section) from beads equilibrated in TMSP solution, and then the inter-bead solution was removed by vacuum suction.

3.2.2 Temperature correction

The temperature inside the rotor increases with spin rate.[43,44] According to Curie's law, signal intensities are approximately inversely proportional to the absolute temperature and must thereby be normalized to each other as

$$I_1 = I_2 \frac{T_2}{T_1} \qquad (2)$$

where I_i are the signal intensities at temperatures T_i, respectively. Because the chemical shift difference between the water and TMSP signals in the spectrum can be used as a sufficiently sensitive internal thermometer (calibrated by performing identical experiments with a sample of 80% ethylene glycol in deuterated dimethyl sulfoxide), the temperature inside the rotor at different MAS spin rates can be measured and its variation corrected for via Eq. (2).

3.2.3 Correcting for the effect of RF field strength

Besides affecting signal intensity as given by Eq. (2), a changing temperature also affects the RF circuit in the probe used for detecting the signal (even when the circuit is optimally tuned and matched at each temperature). If, as a consequence, the effective RF field strength is altered, and if such a change is not accounted for by suitably calibrating and setting the correct pulse length, the signal intensities become lower because the pulse is no longer 90°. An even stronger effect is loss of signal due to – according to the reciprocity principle[41] – decreased receptivity. This latter effect can be corrected for by normalization as

$$I_1 = I_2 \frac{\tau_2}{\tau_1} \qquad (3)$$

where I_i are the signal intensities obtained by 90° pulse lengths τ_i, respectively. The efficiency of these corrective measures is illustrated in Fig. 5 for samples where material re-distribution was shown to have no significant effect (recall Fig. 4). As is clear, the signal level of TMSP is constant, and thereby quantitative experiments are enabled. Tests performed with non-spinning samples at temperatures set to values experienced at the explored spinning rates verified that the main reason for the change in RF efficiency was, indeed, the changing temperature.
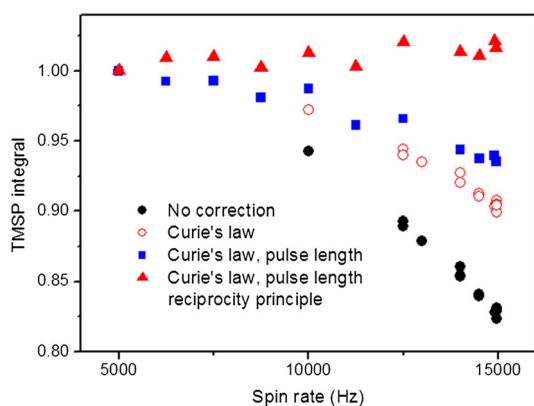
Figure 5. The integral intensity of the 3-(trimethylsilyl)propionic acid (TMSP) signal (normalized to that at 5000 Hz) in samples prepared from beads equilibrated in TMSP solution and then having the inter-bead solution removed by vacuum suction. The symbols represent integrals with no correction (●), corrected for temperature change by Eq. (2) (○), subsequently corrected for RF field change by recording the integrals with 90° pulse length properly calibrated at each spin rate (■), and finally corrected for receptivity change as given by Eq. (3) (▲).

The protocol to obtain accurate ^{1}H HR-MAS intensities

The butyl signals are expected to increase with increasing spin rate both because of more efficient averaging and because the signal intensity distributed to the spinning side bands is progressively relocated to the center band,[23] as discussed in Section 3.1. This latter effect was, however, not so pronounced for our sample because the total intensity of spinning sidebands was decreasing quickly with increasing spin rate and became apparently less than 1% of the center band intensity in the range 5–15 kHz. Hence, the butyl/TMSP integral ratio is not supposed to be influenced by this effect, as has been discussed in Section 3.1. Yet, in bead pack samples prepared via pathway A, we found on some occasions that the increase of the butyl signal integral intensity continued to increase, albeit weekly, over the whole range of explored spin rates. We think this behavior is caused by accidentally removing not only inter-bead but also, by simple drying if the vacuum was kept on too long, some intra-bead solution. In such dry parts, the spectral features are shifted toward that presented in Fig. 3 with accompanying signal loss.

Hence, we resorted to sample preparation via pathway B, where the rotor is only partly filled by a very small volume (10 µl) of slurry with high bead concentration (Section 2.2). In this manner, the sample spreads upon spinning over the rotor wall but in a small enough volume within which the RF inhomogeneity is sufficiently small so that re-distribution of material (that is, beads and solvent) has no significant effect. On the other hand, the sample remained fully hydrated all time. As shown in Fig. 6, we reach after suitable corrections outlined in the previous sub-sections a constant level of TMSP integral and, at spin rate above 13 kHz, the ratio of butyl and TMSP signal integrals also levels off (indicating that the MAS averaging effect of the butyl signals is complete). This behavior was confirmed in repeated runs and repeated sample preparations. It should be noted that it is not enough to limit sample re-distribution in the axial direction (as in commercially available reduced-volume rotors) because the B_1-field is strongly inhomogeneous in the radial direction.[38–40]

Another important advantage provided by pathway B is that there is no solution removal step after having prepared the slurry of medium in TMSP solution. Hence, the TMSP content in relation
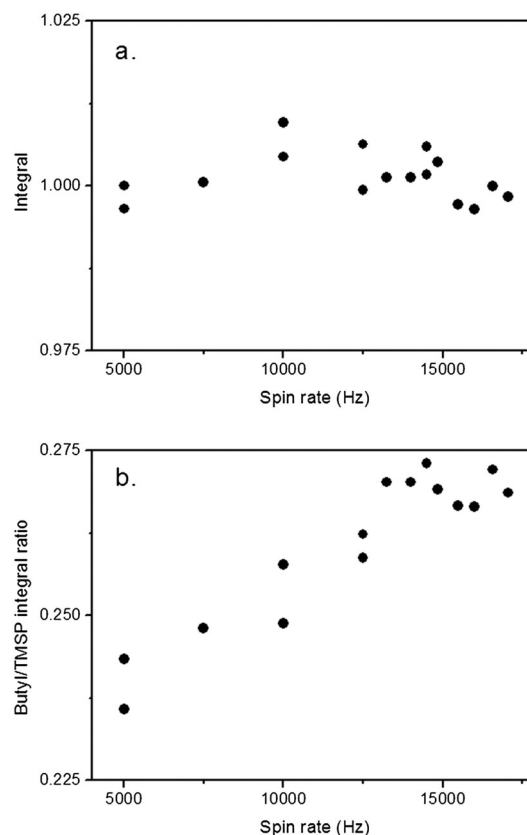

Figure 6. (a) The integral intensity of the 3-(trimethylsilyl)propionic acid (TMSP) signal (normalized to that in one experiment at 5000 Hz) as a function of spin rate in a 10 µl slurry sample partially filling the rotor. The integral presented is corrected for temperature variation by spinning rate and RF-receptivity effects as in Figure 4. (b) The ratio of butyl and TMSP signal integrals as a function of spin rate.

to the bead and ligand content remains constant, irrespective if any interaction of the TMSP with the matrix causes enrichment of TMSP either in the pore space or in the inter-bead bulk solvent.

Precision and accuracy of the developed method

The reproducibility of the method described in Section 3.3 was tested by performing seven replicates where all the steps in the procedure were repeated (preparation of slurry, transfer of 10 µl to the rotor, and acquisition of a spectrum at spin rate 14500 Hz). One prepared sample provided for some reason (assumedly an air bubble) much broader lines than the other samples and far (by over five standard deviations) lower calculated ligand concentration; the result from that preparation was excluded from the analysis in the succeeding discussion. From the obtained butyl and TMSP intensities, the butyl ligand concentration was calculated via Eq. (1). Hence, the result becomes independent on the precision of volume of the transferred 10 µl slurry. The obtained data are shown in Table 1.

It should in addition be noted, though, that there arise some small signals from the resin and the TMSP in the same spectral range as the butyl signals, see inset in Fig. 2c. The two signals at 0.74 and 2.14 ppm originate from non-deuterated methylene groups in TMSP. The former is included in the butyl integration range but gives a very small contribution (~0.2 µmol/ml) to the calculated ligand concentration. The ligand concentrations in

Table 1. Butyl ligand concentration results for replicated measurements using the proposed protocol and calculated via Eq. (1)

Sample	Ligand concentration (μmol/ml)	Average[a]	σ[b]
1	60.2	59.3	1.0
2	61.4		(1.7%)
3	60.5		
4	62.5		
5	60.4		
6	62.1		

[a]Corrected for c_{resin}.
[b]Compounded standard deviation from c_{resin} and the sample-to-sample variation.

Table 1 were corrected for this contribution. The peaks in the 1–1.5 ppm range come from mobile and presumably grafted moieties that were originally in the resin. By analyzing the spectrum of the resin prior to functionalization by the ligand, it is possible to correct for the error introduced by their presence. Integration of the 1–1.5 ppm spectral range in the inset spectrum in Fig. 2c yields that those peaks contributed by $c_{resin} = 1.9 \pm 0.2\,\mu$mol/ml to the detected ligand concentration. The corresponding resin signals in the ^{13}C NMR spectrum caused a similar overestimate of concentration by about 2 μmol/ml.[3] Like in the ^{13}C case,[3] the average concentration presented in Table 1 was corrected for this effect.

We hereby find that ^{1}H HR-MAS yields the average ligand concentration 59.3 μmol/ml with a reproducibility characterized by a standard deviation of 1.0 μmol/ml (1.7% relative standard deviation). Previously,[3] the same ligand concentration was determined, for the same medium lot, to be 58.9 μmol/ml (average of two separate sets of experiments, both with 2% relative standard deviation) by ^{13}C SPE MAS NMR in compressed beads. The excellent agreement between the results presented here and there[3] confirms that any systematic error is small. We note that both here and in the previous paper,[3] we expressed the concentration per unit volume; this arises from the specific requirements for evaluating chromatography media. Measuring mass concentrations simply requires accurate density data such as the ones available for this system.[3]

As illustrated by the spectra in Fig. 2, the scatter of data in Table 1 is not connected to signal-to-noise ratio[45,46]; in fact, that is sufficient even in one or two scans in the sense that it will not significantly decrease precision. In other word, the origin of precision is either instrumental instability or variation among samples or both. Considering that the total time for preparation (as described in Section 3.3, and rotor insertion in the probe) of a single sample is ~5–6 min, the total experimental time necessary is below 10 min.

Conclusions

We present here a precise and accurate – the latter indicated by the agreement with the results presented previously[3] – method for measuring the ligand concentration in hydrated Butyl Sepharose High Performance chromatography media with ^{1}H HR-MAS NMR spectroscopy. Hydration leads to relatively mobile butyl ligands and that, in turn, leads to signal integrals that are accurate at sufficiently low (in our case, around 15 kHz) of spinning speed. Accuracy also required that one corrected for small temperature

effects, both direct (that is, change in nuclear magnetization) and indirect (change in probe RF properties). Finally, it is essential to use protocols for sample preparation and for filling the sample holders on a manner that reduces errors caused by irreproducibility and sample re-distribution. The remaining errors are largely due to these latter factors. The developed final protocol, termed earlier as pathway B, also provides a simple way to relate the obtained volume concentration of ligands to the same quantity in real chromatography columns where the medium is compressed. In addition, the protocol is not sensitive to interaction between the selected reference molecule and the matrix that may cause local (within the pore space or within the bulk liquid among the beads, depending on the nature of the interaction involved) enrichment of the reference in the solvent. For the same reason, it is also applicable to matrices of different pore sizes.

We believe that the method presented here can be applied for a number of different analytes, such as other chromatography media and ligands, porous media, and, assumedly, tissue samples[9,47–49] and has thereby the potential to find wider application. A clear limiting factor is the molecular mobility of the moiety one wishes to investigate. If that is low, the spinning speed available at the spectrometer of choice may not be sufficient to reach the limiting value of the spectral intensity of the relevant central peaks in the MAS spectra. In this context, note that currently 70 kHz spinning speeds are becoming widespread. Hence, this shortcoming may turn out to be less important in the future. Effects of sample redistribution could be further limited by using suitable cylindrical rotor inserts that exclude the volume closest to the rotor wall, the region where RF inhomogeneity is highest.[40]

We also note that the two methods, the one presented here and the other previously,[3] do not have optimal performance for the same dynamical regime of the target molecules – the ^{13}C SPE method performed best in sparsely hydrated samples where the ^{1}H HR-MAS method was not working at all. Having both methods presented and analyzed permits others to choose the protocol best adjusted to their particular system. An advantage of the ^{13}C SPE method is its high spectral resolution, which probably renders it being more generally applicable for quantitative analysis. On the other hand, once established for a particular sort of material, the ^{1}H HR-MAS method is far quicker, which awards it an unparalleled potential in, for example, quality and process control.

References

[1] C. R. Cantor, *Protein Purification – Principles and Practice*, Springer, New York, **1994**.
[2] J. C. Jansson, L. Rydén, *Protein Purification*, Wiley, New York, **1998**.
[3] F. Elwinger, S. V. Dvinskikh, I. Furó. *Magn. Reson. Chem.* **2015**, *53*, 572–577.
[4] I. Drevin, B. L. Johansson. *J. Chromatogr.* **1984**, *295*, 210–214.
[5] B. L. Johansson, I. Drevin. *J. Chromatogr.* **1985**, *321*, 335–342.
[6] B. L. Johansson, I. Drevin. *J. Chromatogr.* **1985**, *346*, 255–263.
[7] B. L. Johansson, I. Drevin. *J. Chromatogr.* **1987**, *391*, 448–451.
[8] A. Berggrund, I. Drevin, K. G. Knuuttila, J. Wardhammar, B. L. Johansson. *Process Biochem.* **1994**, *29*, 455–463.

[9] C. K. Larive, G. A. Barding, M. M. Dinges. *Anal. Chem.* **2015**, *87*, 133–146.

[10] K. Paradowska, I. Wawer. *J. Pharm. Biomed. Anal.* **2014**, *93*, 27–42.

[11] G. F. Pauli, B. U. Jaki, D. C. Lankin. *J. Nat. Prod.* **2005**, *68*, 133–149.

[12] W. L. Fitch, G. Detre, C. P. Holmes, J. N. Shoolery, P. A. Keifer. *J. Org. Chem.* **1994**, *59*, 7955–7956.

[13] M. Coen, I. D. Wilson, J. K. Nicholson, H. Tang, J. C. Lindon. *Anal. Chem.* **2004**, *76*, 3023–3028.

[14] S. K. Sarkar, R. S. Garigipati, J. L. Adams, P. A. Keifer. *J. Am. Chem. Soc.* **1996**, *118*, 2305–2306.

[15] M. Pursch, L. C. Sander, H. J. Egelhaaf, M. Raitza, S. A. Wise, D. Oelkrug, K. Albert. *J. Am. Chem. Soc.* **1999**, *121*, 3201–3213.

[16] S. Bachmann, C. Hellriegel, J. Wegmann, H. Handel, K. Albert. *Solid State Nucl. Magn. Reson.* **2000**, *17*, 39–51.

[17] U. Skogsberg, H. Handel, D. Sanchez, K. Albert. *J. Chromatogr. A* **2004**, *1023*, 215–223.

[18] U. Skogsberg, C. Meyer, J. Rehbein, G. Fischer, S. Schauff, N. Welsch, K. Albert, A. J. Hall, B. Sellergren. *Polymer* **2007**, *48*, 229–238.

[19] S. Schauff, V. Friebolin, M. D. Grynbaum, C. Meyer, K. Albert. *Anal. Chem.* **2007**, *79*, 8323–8326.

[20] V. Friebolin, S. Marten, K. Albert. *Magn. Reson. Chem.* **2010**, *48*, 111–116.

[21] H. Yeman, T. Nicholson, M. T. Matyska, J. J. Pesek, K. Albert. *J. Sep. Sci.* **2013**, *36*, 173–181.

[22] V. Friebolin, M. P. Bayer, M. T. Matyska, J. J. Pesek, K. Albert. *J. Sep. Sci.* **2009**, *32*, 1722–1728.

[23] C. A. Fyfe, *Solid State NMR for Chemists*, C.F.C. Press, Guelph, Ontario, **1983**.

[24] M. J. Albers, T. N. Butler, I. Rahwa, N. Bao, K. R. Keshari, M. G. Swanson, J. Kurhanewicz. *Magn. Reson. Med.* **2009**, *61*, 525–532.

[25] K. Millis, P. Weybright, N. Campbell, J. A. Fletcher, C. D. Fletcher, D. G. Cory, S. Singer. *Magn. Reson. Med.* **1999**, *41*, 257–267.

[26] M. G. Swanson, A. S. Zektzer, Z. L. Tabatabai, J. Simko, S. Jarso, K. R. Keshari, L. Schmitt, P. R. Carroll, K. Shinohara, D. B. Vigneron, J. Kurhanewicz. *Magn. Reson. Med.* **2006**, *55*, 1257–1264.

[27] R. Warrass, G. Lippens. *J. Org. Chem.* **2000**, *65*, 2946–2950.

[28] L. L. Cheng, C. L. Wu, M. R. Smith, R. G. Gonzalez. *FEBS Lett.* **2001**, *494*, 112–116.

[29] L. H. Lucas, M. A. Cerny, Y. M. Koen, R. P. Hanzlik, C. K. Larive. *Anal. Bioanal. Chem.* **2004**, *380*, 627–631.

[30] J. L. Taylor, C. L. Wu, D. Cory, R. G. Gonzalez, A. Bielecki, L. L. Cheng. *Magn. Reson. Med.* **2003**, *50*, 627–632.

[31] C. L. Wu, J. L. Taylor, W. L. He, A. G. Zepeda, E. F. Halpern, A. Bielecki, R. G. Gonzalez, L. L. Cheng. *Magn. Reson. Med.* **2003**, *50*, 1307–1311.

[32] J. Blas, A. Rivera-Sagredo, R. Ferritto, J. F. Espinosa. *Magn. Reson. Chem.* **2004**, *42*, 950–954.

[33] R. Hany, D. Rentsch, B. Dhanapal, D. Obrecht. *J. Comb. Chem.* **2001**, *3*, 85–89.

[34] B. R. Cohn, B. N. Joe, S. J. Zhao, J. Kornak, V. Y. Zhang, R. Iman, J. Kurhanewicz, K. Vahidi, J. W. Yu, A. B. Caughey, M. G. Swanson. *Magn. Reson. Mater. Phys., Biol. Med.* **2009**, *22*, 343–352.

[35] F. Ziarelli, S. Caldarelli. *Solid State Nucl. Magn. Reson.* **2006**, *29*, 214–218.

[36] F. Ziarelli, S. Viel, S. Sanchez, D. Cross, S. Caldarelli. *J. Magn. Reson.* **2007**, *188*, 260–266.

[37] M. C. Martínez-Bisbal, D. Monleon, O. Assemat, M. Piotto, J. Piquer, J. L. Llácer, B. Celda. *NMR Biomed.* **2009**, *22*, 199–206.

[38] N. C. Nielsen, H. Bildsöe, H. J. Jakobsen. *J. Magn. Reson.* **1992**, *98*, 665–673.

[39] K. Elbayed, B. Dillmann, J. Raya, M. Piotto, F. Engelke. *J. Magn. Reson.* **2005**, *174*, 2–26.

[40] J. Mispelter, M. Lupu. *C. R. Chimie* **2008**, *11*, 340–355.

[41] D. I. Hoult, R. E. Richards. *J. Magn. Reson.* **1976**, *24*, 71–85.

[42] Y. Q. Song. *J. Magn. Reson.* **2000**, *143*, 397–401.

[43] J. Brus. *Solid State Nucl. Magn. Reson.* **2000**, *16*, 151–160.

[44] S. V. Dvinskikh, V. Castro, D. Sandström. *Magn. Reson. Chem.* **2004**, *42*, 875–881.

[45] C. Rischel. *J. Magn. Reson. A* **1995**, *116*, 255–258.

[46] S. Bourg, J. M. Nuzzillard. *J. Magn. Reson.* **1998**, *134*, 184–188.

[47] M. Andre, J. N. Dumez, L. Rezig, L. Shintu, M. Piotto, S. Cadarelli. *Anal. Chem.* **2014**, *86*, 10749–10754.

[48] B. Sitter, T. F. Bathen, M. B. Tessem, I. S. Gribbestad. *Prog. Nucl. Magn. Reson. Spectrosc.* **2009**, *54*, 239–254.

[49] E. C. Y. Chan, P. K. Koh, M. Mal, P. Y. Cheah, K. W. Eu, A. Backshall, R. Cavill, J. K. Nicholson, H. C. Keun. *J. Proteome Res.* **2009**, *8*, 352–361.